Kosterlitz-Thouless transition in planar spin models with bond dilution

Tasrief Surungan*
Department of Physics, Hasanuddin University, Makassar 90245, Indonesia
and Department of Physics, Tokyo Metropolitan University, Hachioji, Tokyo 192-0397, Japan

Yutaka Okabe†
Department of Physics, Tokyo Metropolitan University, Hachioji, Tokyo 192-0397, Japan
(Received 12 January 2005; published 31 May 2005)

We study the two-dimensional bond-diluted *XY* and six-state clock models by Monte Carlo simulation with cluster spin updates. Various concentrations of depleted bonds were simulated, in which we found a systematic decrease of the Kosterlitz-Thouless (KT) transition temperatures of both *XY* and six-state clock models as the concentration of dilution decreases. For the six-state clock model, a second KT transition at lower temperature was observed. The KT transition temperatures as well as the decay exponent η for each concentration of dilution are estimated. It is observed that the quasi-long-range order disappears at the concentration of dilution very close to the percolation threshold. The decay exponent η of the KT transitions calculated at each concentration indicates that the universality class belongs to the pure *XY* and clock models, analogous to the expectation of the Harris criterion for the irrelevance of randomness in the continuous phase transition of systems with nondiverging specific heat.

DOI: 10.1103/PhysRevB.71.184438 PACS number(s): 75.50.Lk, 75.10.Hk, 64.60.Fr, 05.70.Jk

I. INTRODUCTION

Dilution is an indispensable aspect of both theoretical and experimental studies due to the presence of defects and impurities in any real material.[1,2] The pioneering work by Harris[3] on the effect of dilution on the critical behavior of systems with continuous transition has stimulated many studies in the field of random systems. Based on the Harris criterion, it is predicted that the dilution will be relevant (irrelevant) if the specific heat exponent α of the pure system is positive (negative), and becomes marginal in the case $\alpha=0$, for example, in the two-dimensional (2D) Ising system.[4]

It is well known that the pure 2D *XY* model cannot have a true long-range order at any finite temperature due to the continuous symmetry $U(1)$.[5,6] However, the system can exist in a quasi-long-range order (QLRO), an intermediate phase which is a topological excitation formed by vortex-antivortex pairs.[7] The number of vortex-antivortex pairs increases with the temperature until the system experiences the Kosterlitz-Thouless (KT) transition. This transition corresponds to the unbinding of vortex-antivortex pairs, which leads the system to a high-temperature disordered phase.

The existence of QLRO in the presence of dilution is an interesting topic. This is related to the fact that the QLRO is a topological order vulnerable to the local defect or perturbation. The diluted *XY* models may have relevance to the study of superconductivity, in particular the interaction between vortices and the spatial inhomogeneity due to the impurities. However, not so much attention has been paid to the dilution effect on the KT transition.

Quite recently, two contradictory results on the 2D site diluted *XY* model were reported.[8,9] By using the Monte Carlo (MC) simulation with the Metropolis algorithm, Leonel *et al.*[8] showed that the QLRO disappears before the concentration of vacant sites reaches the percolation threshold p_c of site dilution. On the other hand, performing a more extensive MC study with the Wolff cluster algorithm,[10] Berche *et al.*[9] suggested that the QLRO remains up to dilute concentration very close to the percolation threshold p_c (for the site dilution on the square lattice $p_c \sim 0.593$). With these two inconsistent results, it is worth carrying out a detailed study of the dilution problem from a different point of view. Here, treat a bond-diluted case; it should be made clear whether or not the QLRO remains up to the percolation threshold of bond dilution.

The effect of the q-fold symmetry-breaking fields on the 2D *XY* model has been the subject of attention.[11,12] Treating clock models, where only discrete angles of the *XY* spins are allowed, is essentially equivalent to probing the q-fold symmetry-breaking fields. The $U(1)$ symmetry of the *XY* model is replaced by the discrete Z_q symmetry in the q-state clock model. It was shown[11] that the 2D q-state clock model has two phase transitions of KT type at T_1 and $T_2 (T_1 < T_2)$ for $q > 4$. There is an intermediate *XY*-like QLRO phase between a low-temperature ordered phase ($T < T_1$) and a high-temperature disordered phase ($T > T_2$). The effect of dilution on the low-temperature ordered phase due to the discrete symmetry of the clock model is another interesting subject to study.

In this paper, we study the bond-diluted *XY* and six-state clock models ($q=6$) on the square lattice. We use the Monte Carlo method with cluster flip. For the estimator of the KT transition we use the ratio of magnetic correlation functions with different distances.[13] In the next section, we describe our model and the detail of calculation method. Then, in Sec. III we shall present our results. Section IV is devoted to the summary and concluding remarks. A part of the preliminary results of the present work was reported at the conference, "Statistical Physics of Disordered Systems and its Application," which was held in July 2004, at Hayama, Japan.[14]

II. MODEL AND SIMULATION METHOD

The bond-diluted XY spin model is written with the Hamiltonian

$$H = \sum_{\langle ij \rangle} J_{ij} \boldsymbol{S}_i \cdot \boldsymbol{S}_j = \sum_{\langle ij \rangle} J_{ij} \cos(\theta_i - \theta_j), \tag{1}$$

where summation is performed over the whole nearest-neighbors pairs $\langle ij \rangle$, $\boldsymbol{S}_i$ being a unit planar spin vector occupying the ith site of lattice system (here, we deal with the square lattice), and θ_i the angle associated with the ith spin. For the six-state clock model, the angle takes discrete values, $\theta_i = 2\pi q/6$ with $q = 0,\ldots,5$. The quenched dilution is conveyed by the coupling J_{ij} following a distribution $P(J_{ij}) = p\,\delta(J_{ij} - J) + (1-p)\,\delta(J_{ij})$, with p being the concentration of existing bonds, or we can say $(1-p)$ is the concentration of the diluted (missing) bonds.

We make use of the canonical sampling MC method with multicluster spin updates (Swendsen-Wang algorithm[15]). The embedded cluster idea for continuous spins due to Wolff[10] is adopted, namely by projecting the planar spins into a random axis so that the Kasteleyn-Fortuin[16] procedure on Ising spins can be performed. Spins with missing bonds due to dilution are not connected in forming a cluster.

We simulated the 2D diluted XY and six-state clock models on the square lattice with periodic boundary conditions. We treated both models with the linear sizes of $L = 32$, 48, 64, 80, and 96. Various bond concentrations, from the pure case $p = 1.0$ down to $p = 0.55$, were simulated. For each concentration of each system size we treated many different realizations in order to get better statistics; typical number of realizations is 256, except for $p = 0.55$, where more realizations were taken into account to compensate highly sample-dependent results. We performed 10^4 MC steps for the equilibration and 4×10^4 MC steps for the measurement. We use the reweighting technique[17] to obtain the thermal average at temperatures different from those at which actual simulations were made.

III. RESULTS

A. Specific heat

Let us start by presenting the results of the specific heat for the diluted XY and six-state clock models on the square lattice. The specific heat per spin is defined as follows:

$$C(T) = \frac{1}{NkT^2}[\langle E^2 \rangle - \langle E \rangle^2], \tag{2}$$

where k is the Boltzmann constant. The number of spins and the total energy are denoted by N and E, respectively.

The temperature dependence of specific heat for various bond concentrations is plotted in Fig. 1 for the diluted XY and six-state clock models. The temperature is represented in units of J/k from now on. The statistical errors are less than the order of the width of curves. We see that the size dependence is small, which is typical for the KT transition. Single finite peaks observed in the diluted XY model may correspond to the existence of one KT transition; on the other hand there are double peaks for the diluted clock models, which signify the existence of two KT transitions. In both models, the positions of the peaks gradually shift to the lower temperature as we reduce the bond concentration; the peaks become relatively flat with the decrease of p. This indicates that the QLRO in the system gradually fades away. However, no abrupt change has been observed; the change with p is smooth and continuous. More quantitative analysis on the critical behavior shall be performed on the magnetic correlation ratio in the following.

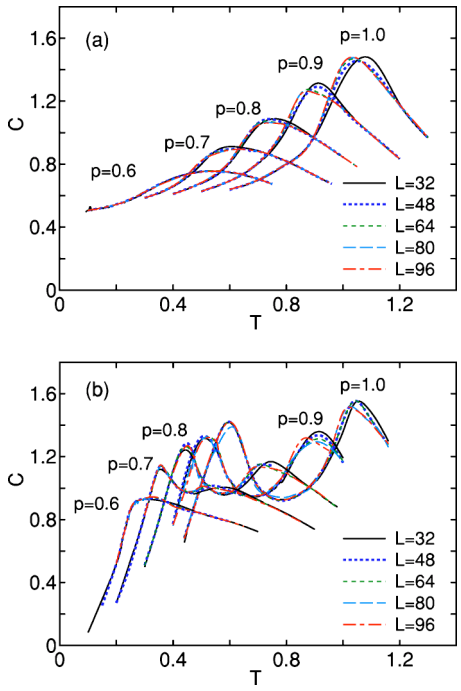

FIG. 1. (Color online) Temperature dependence of specific heat of the diluted (a) XY and (b) six-state clock models for various bond concentrations of system sizes $L = 32$, 48, 64, 80, and 96.

B. Magnetic correlation ratio

The critical behavior of magnetic ordering can be investigated more precisely from the evaluation of the magnetic correlation function which is defined as the following:

$$g(r) = \langle \boldsymbol{S}_i \cdot \boldsymbol{S}_{i+r} \rangle, \tag{3}$$

where r is the fixed distance between spins. Precisely, the distance r is a vector, but we have used a simplified notation.

Consider the ratio of the correlation functions with different distances. At the critical point or on the critical line, the correlation function $g(r)$ for an infinite system decays as a power of r

$$g(r) \sim r^{-(D-2+\eta)}, \tag{4}$$

where D is the spatial dimension and η the decay exponent. For a finite system in the critical region, it can be shown that the ratio of the correlation functions with different distances has a finite-size scaling (FSS) form with a single scaling variable

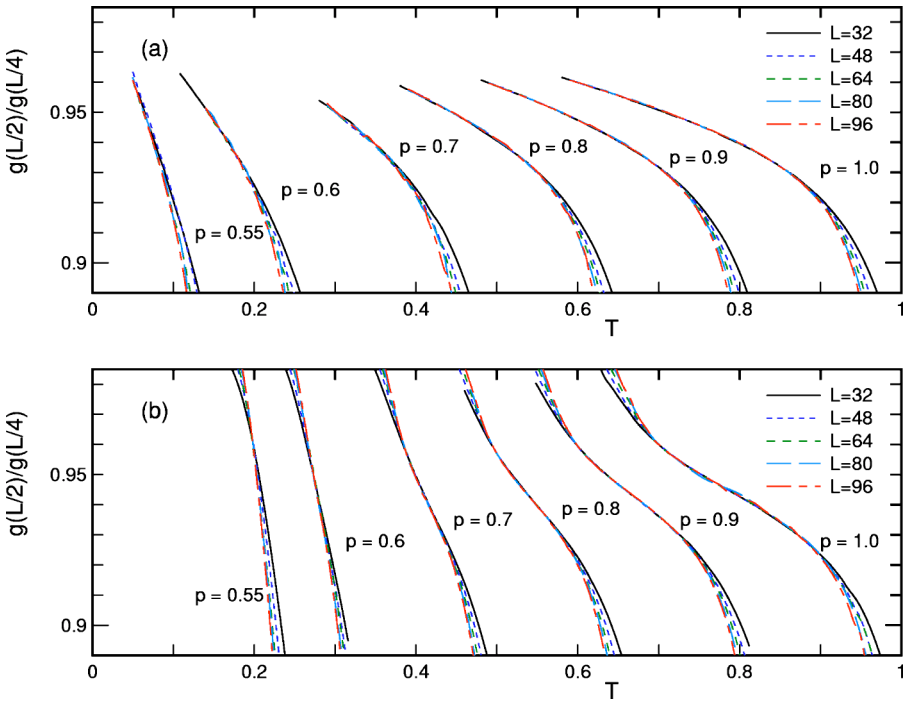

FIG. 2. (Color online) Ratio of magnetic correlation functions of the diluted (a) *XY* and (b) six-state clock models for various bond concentrations of sizes $L=32$, 48, 64, 80, and 96. The temperature is represented in units of J/k.

$$\frac{g(r,t,L)}{g(r',t,L)} = f(L/\xi), \tag{5}$$

if we fix two ratios, r/L and r/r', where ξ is the correlation length.

Tomita and Okabe[13] showed that this correlation ratio with different distances is a very good estimator for the analysis of the second-order phase transition, as well as for the KT transition. The helicity modulus[18] and the Binder parameter[19] are often used in the analysis of the KT transition, but the correlation ratio is more efficient in the sense that corrections to FSS are smaller.[13] It has been successfully applied to the study of the 2D fully frustrated clock model.[20]

In the present work, we consider the ratio of magnetic correlation functions setting $r=L/2$ and $r'=L/4$ for two distances. Thus, we evaluate the correlation ratios $g(L/2)/g(L/4)$.

1. Estimate of KT transition temperatures

We show the temperature dependence of magnetic correlation ratio for various bond concentrations p in Fig. 2 for the diluted *XY* and six-state clock models. The data of different sizes for each bond concentration are plotted. The statistical errors are less than the order of the width of curves. Although at high temperatures curves of different sizes are separated, they gradually merge as the temperature is decreased. At lower temperatures the curves of different sizes are collapsed on a single curve, which is the behavior of the QLRO phase, in other words, on the critical line. The essential feature of the diluted systems is the same as the pure case, which indicates the existence of the KT transition. The approach to QLRO phase is described by the scaling behavior shown in Eq. (5). For the six-state clock model, the curves with different sizes separate again at low enough temperatures. This comes from the discrete symmetry of the clock model, which yields the low-temperature ordered phase. Thus, in addition to the high-temperature KT transition, a second KT transition at lower temperature exists for the six-state clock model. We find that the overall behavior of the diluted clock model is essentially the same as the pure clock model, except that the KT transition temperatures decrease with the dilution. We shall estimate the KT transition temperatures of both the *XY* and clock models using FSS.

With the FSS analysis based on Eq. (5) and the KT form of the correlation length, $\xi \propto \exp(c/\sqrt{t})$, where $t=|T-T_{\mathrm{KT}}|/T_{\mathrm{KT}}$, we can write the L dependence of $T_{\mathrm{KT}}(L)$ as follows:

$$T_{\mathrm{KT}}(L) = T_{\mathrm{KT}} + \frac{c^2 T_{\mathrm{KT}}}{(\ln bL)^2}. \tag{6}$$

We consider the size-dependent critical temperature $T_{\mathrm{KT}}(L)$ that gives the constant $R=g(L/2)/g(L/4)$. In Fig. 3, we show the plot of $T_{\mathrm{KT}}(L)$ as a function of l^{-2}, with $l=\ln(bL)$, using best-fitted parameters b and c for the diluted *XY* and six-state clock models with $p=0.9$. The system sizes are $L=32$, 48, 64, 80, and 96. For the value of R, 0.600, 0.650, and 0.700 are used for the *XY* model, and $T_{\mathrm{KT}}(L)$ obtained using different R are represented by different marks. For the estimate of T_2 of the diluted clock model, the value of R is set to be 0.600, 0.650, and 0.700, whereas R is 0.975, 0.985, and 0.995 for T_1. The data using different R are collapsed on a single curve, which suggests that the difference of R is absorbed in the R dependence of b. The intercepts in the vertical axis of Fig. 3 give the estimate of the KT transition temperatures. The estimate of T_{KT} for the diluted *XY* model with $p=0.9$ is 0.747(4). The number in the parentheses denotes the uncertainty in the last digits. In the same way, we estimate the two KT transition temperatures of the diluted six-state clock model, T_2 and T_1, as 0.727(4) and 0.605(4), respectively.

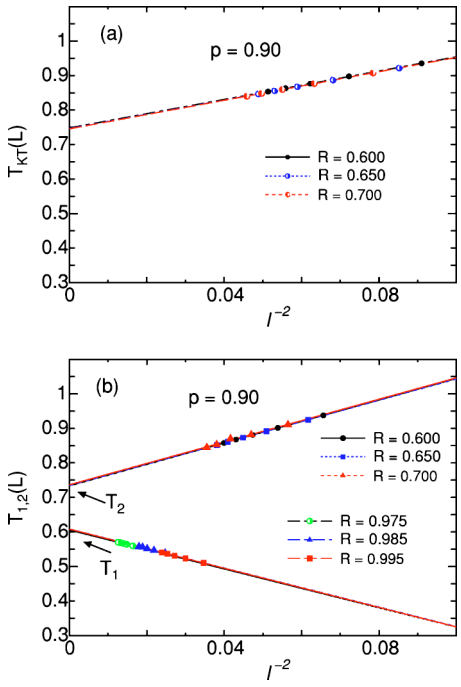

FIG. 3. (Color online) The plot of $T_{KT}(L)$ versus l^{-2}, with $l = \ln bL$, to estimate KT transition temperature of the diluted (a) *XY* and (b) six-state clock models on the square lattice for $L=32$, 48, 64, 80, and 96, with bond concentration $p=0.9$. For the clock model, both the higher (T_2) and lower (T_1) KT transition temperatures are estimated. The data obtained from different values of R are shown by different marks.

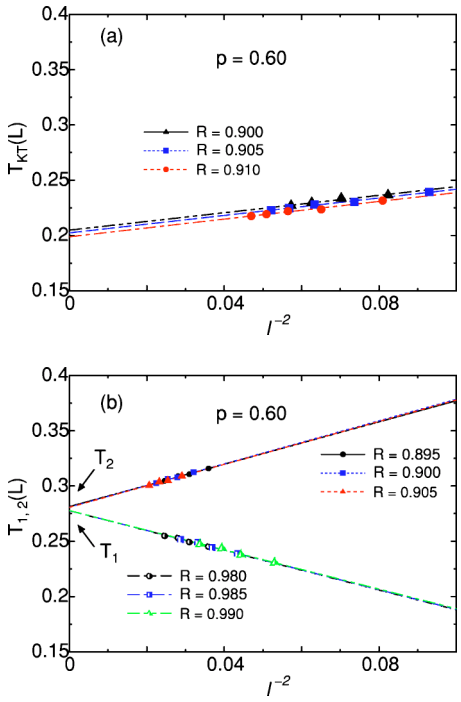

FIG. 4. (Color online) The plot of $T_{KT}(L)$ versus l^{-2}, with $l = \ln bL$, to estimate KT transition temperature of the diluted (a) *XY* and (b) six-state clock models on the square lattice for $L=32$, 48, 64, 80, and 96, with bond concentration $p=0.6$. For the clock model, both the higher (T_2) and lower (T_1) KT transition temperatures are estimated. The data obtained from different values of R are shown by different marks.

We also plot the data for $p=0.6$ in Fig. 4. The choice of fixed R is different from that for $p=0.9$. The estimated KT transition temperatures are given by the intercepts in the vertical axis. The KT transition temperatures for $p=0.6$ are lower than those for $p=0.9$; for the six-state clock model the QLRO phase between T_1 and T_2 becomes narrower.

Performing the same procedure for other bond concentrations, we estimate their KT transition temperatures; they are tabulated in Table I. For the six-state clock model, the lower (T_1) and higher (T_2) KT transition temperatures are estimated. In Fig. 5 we show the phase diagram of the diluted systems, which is produced from Table I. As can be seen from the phase diagram, the KT transition temperatures gradually decrease with dilution, and the QLRO phase disappears at the bond concentration which is very close to the percolation threshold p_c; for the bond percolation of the square lattice, $p_c=0.5$. This result is the same as that of Berche *et al.*[9] for the site dilution, but different from that of Leonel *et al.*[8]

For the clock model the intermediate QLRO phase is suppressed to a narrow range of temperature as the diluted bonds increase. The lower KT transition comes from the discrete symmetry. Thus, the behavior near the percolation threshold is similar to the case of the diluted Ising model. The higher KT transition temperature T_2 for the clock model becomes higher than T_{KT} for the *XY* model with the same p near $p=0.5$, which may be related to the stabilization effect of discrete symmetry.

2. Decay exponent

Next, we consider the decay exponent η of both *XY* and six-state clock models for each bond concentration. We first look at the constant value of correlation ratio R for different sizes and find the associate correlation function $g(L/2)$. We give our attention to the power-law dependence of the correlation function on the system size, $g(L/2) \sim L^{-\eta}$, expressed in Eq. (4) with $D=2$. Choosing the fixed R, we have the same temperature for different sizes on the critical point or on the critical line. Moreover, away from the critical points the same R gives different temperatures for different sizes,

TABLE I. The estimates of KT transition temperatures for the diluted *XY* and six-state clock models for various bond concentration p. For the clock model the lower (T_1) and higher (T_2) KT transition temperatures are estimated.

	XY	Six-state clock	
p	T_{KT}	T_1	T_2
1.0	0.895(3)	0.715(3)	0.902(3)
0.9	0.747(4)	0.605(4)	0.727(4)
0.8	0.575(6)	0.489(6)	0.574(4)
0.7	0.401(6)	0.388(6)	0.434(6)
0.6	0.215(12)	0.277(4)	0.281(4)
0.55	0.076(8)	0.198(8)	0.204(6)

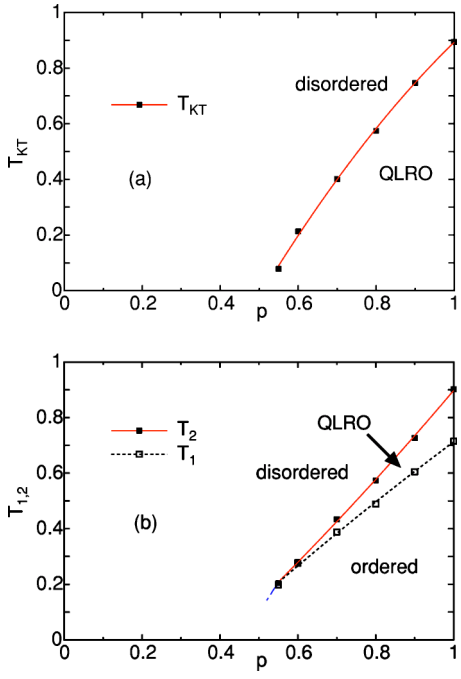

FIG. 5. (Color online) Phase diagram of the diluted (a) *XY* and (b) six-state clock models. As shown, there is a systematic shift of the KT transition temperatures as the bond concentration decreases. The plot suggests that the critical dilution is close to the percolation threshold $p_c=0.5$. For the clock model, due to the discrete symmetry, there exists a lower KT transition, separating the ordered phase of low temperature from the intermediate QLRO.

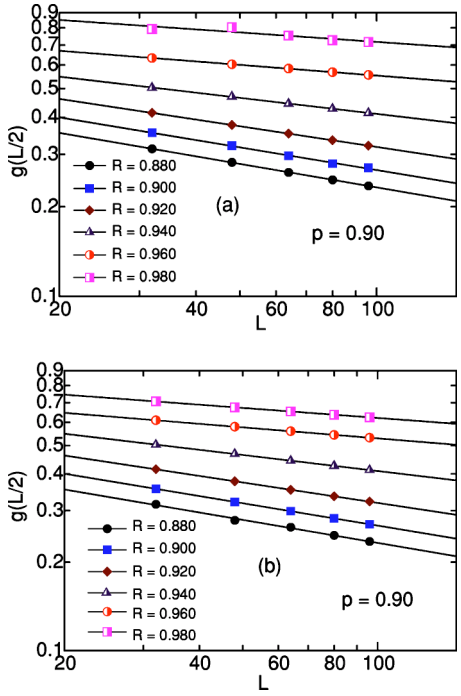

FIG. 6. (Color online) Double-logarithmic plot of the magnetic correlation function $g(L/2)$ versus L of the diluted (a) *XY* and (b) six-state clock models, for bond concentration $p=0.9$. Here, the slope of the best-fitted line of each corresponding R gives the estimate of the exponent η.

but the corrections to the power-law behavior, Eq. (4), are the same, which yields the estimate of the decay exponent η. This analysis of η was used in the study of the fully frustrated clock model.[20] As an example, we consider the system with bond concentration $p=0.9$. We plot $g(L/2)$ versus L for various Rs in double-logarithmic scale for the diluted *XY* and six-state clock models in Fig. 6. The value of η is estimated from the slope of the best-fitted line for each value of constant correlation ratio. Similar plots for $p=0.6$ are given in Fig. 7.

The R dependence of thus-obtained η of each bond concentration for the diluted *XY* and six-state clock models is plotted in Fig. 8. As can be seen, the exponents η of bond diluted system with various bond concentrations behave similar to those of the pure case, $p=1$, namely continuously changing with the temperature in the KT phase. We have plotted the data down to $p=0.6$. All the data seem to be universal, and the corrections are small except for the larger R side of the clock model with $p=0.6$. The deviations from the pure value become larger for $p=0.55$; they are not plotted here. This comes from the fact that it is close to the percolation threshold and corrections become larger. In the renormalization-group language, the critical behavior is affected by another fixed point nearby.

Since the estimated η is almost constant for smaller R, which corresponds to higher temperature, in Fig. 8, the exponent at T_{KT} of the *XY* model and T_2 of the clock model are estimated as

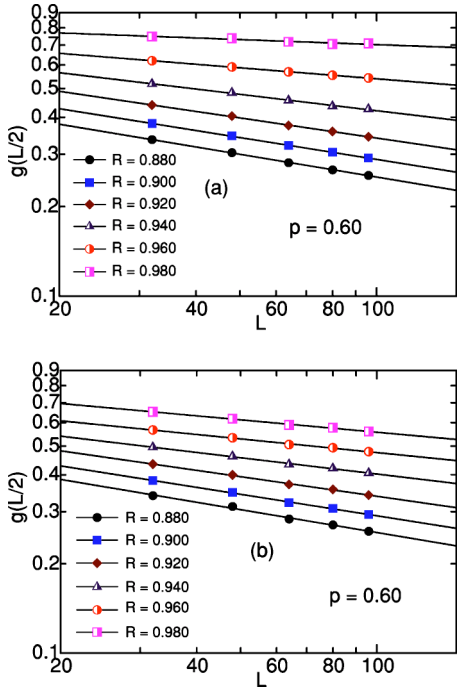

FIG. 7. (Color online) Double-logarithmic plot of the magnetic correlation function $g(L/2)$ versus L of the diluted (a) *XY* and (b) six-state clock models, for bond concentration $p=0.6$. Here, the slope of the best-fitted line of each corresponding R gives the estimate of the exponent η.

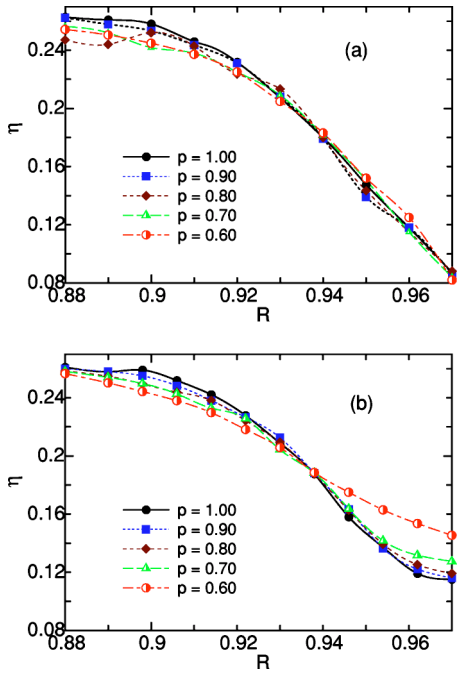

FIG. 8. (Color online) Decay exponent η as function of correlation ratio R of the diluted (a) XY and (b) six-state clock models for various concentrations.

$$\eta_2 = 0.25(1).$$

This value is consistent with that for the pure case, $1/4 = 0.25$. For the low-temperature side (large R) of the XY model, η approaches 0. Meanwhile, the estimated η for the six-state clock model becomes constant for large R. This gives the decay exponent at the lower KT transition temperature T_1 as

$$\eta_1 = 0.12(1),$$

which is consistent with the pure value of $1/9 = 0.111$. The present results suggest that the exponents associated with the KT transitions are universal with dilution.

IV. CONCLUDING REMARKS

In summary, we have investigated the bond dilution of the XY and six-state clock models on the square lattice using the canonical sampling MC method with cluster spin updates. We have observed the KT transition of higher temperature separating the intermediate QLRO phase from the disordered phase. Due to the discrete symmetry of the clock model, the lower KT transition also has been observed. There is a systematic decrease in KT transition temperatures as the concentration of diluted bonds increases. Our estimates of the KT transition temperatures for each concentration, both for the XY and six-state clock models, are listed in Table I, from which the corresponding phase diagram shown in Fig. 5 follows. As can be seen from the phase diagram, the critical concentration of dilution is very close to the percolation threshold, which is the same as the result of Berche *et al.*[9] for the site dilution, but different from that of Leonel *et al.*[8] The bond-diluted and site-diluted classical spin systems show essentially the same behavior, although there may be differences for the quantum spin models.[21,22] Our preliminary results for the site-diluted XY and clock models give the continuous phase transition with respect to p. Thus, our result is in favor of that of Berche *et al.*[9]

The phase diagram also shows that the intermediate QLRO phase for the clock model is suppressed to a narrow range of temperature as the diluted bonds increase. Our estimates of decay exponents for lower concentration dilution suggest that the KT transition remains unaffected by dilution, which is analogous to the expectation of the Harris criterion that the randomness is irrelevant for system with nondiverging specific heat.

Quite recently, Sasamoto and Nishimori have studied the phase diagram of 2D random Z_q models using the duality argument.[23] The analysis of the duality argument for the present model will be left as a future problem.

ACKNOWLEDGMENTS

The authors wish to thank N. Kawashima, H. Otsuka, C. Yamaguchi, Y. Tomita, M. Ito, H. Nishimori, and T. Sasamoto for valuable discussions. One of the authors (T.S.) gratefully acknowledges the support provided by the Ministry of Education, Science, Sports and Culture, Japan. This work was supported by a Grant-in-Aid for Scientific Research from the Japan Society for the Promotion of Science. The computation of this work has been done using the computer facilities of Tokyo Metropolitan University and those of the Supercomputer Center, Institute for Solid State Physics, University of Tokyo.

*Electronic address: tasrief@unhas.ac.id
†Electronic address: okabe@phys.metro-u.ac.jp

[1] R. B. Stinchcombe, *Phase Transition and Critical Phenomena*, edited by C. Domb and M. S. Green (Academic, New York, 1983), Vol. 7.
[2] V. Dotsenko, *Introduction to the Replica Theory of Disordered Statistical Systems* (Cambridge University Press, Cambridge, 2001).
[3] A. B. Harris, J. Phys. C **7**, 1671 (1974).
[4] Y. Tomita and Y. Okabe, Phys. Rev. E **64**, 036114 (2001).
[5] N. D. Mermin and H. Wagner, Phys. Rev. Lett. **17**, 1133 (1966).
[6] P. C. Hohenberg, Phys. Rev. **158**, 383 (1967).
[7] J. Kosterlitz and D. Thouless, J. Phys. C **6**, 1181 (1973); J. M. Kosterlitz, *ibid.* **7**, 1046 (1974).
[8] S. A. Leonel, P. Zimmermann Coura, A. R. Pereira, L. A. S. Mol, and B. V. Costa, Phys. Rev. B **67**, 104426 (2003).
[9] B. Berche, A. I. Farinas-Sanchez, Yu. Holovatch, and R. Paredes V, Eur. Phys. J. B **36**, 91 (2003).

[10] U. Wolff, Phys. Rev. Lett. **62**, 361 (1989).
[11] J. V. José, L. P. Kadanoff, S. Kirkpatrick, and D. R. Nelson, Phys. Rev. B **16**, 1217 (1977).
[12] Y. Tomita and Y. Okabe, Phys. Rev. B **65**, 184405 (2002).
[13] Y. Tomita and Y. Okabe, Phys. Rev. B **66**, 180401(R) (2002).
[14] Y. Okabe and T. Surungan, Prog. Theor. Phys. Suppl. (to be published).
[15] R. H. Swendsen and J.-S. Wang, Phys. Rev. Lett. **58**, 86 (1987).
[16] P. W. Kasteleyn and C. M. Fortuin, J. Phys. Soc. Jpn. **26**, 11 (1969); C. M. Fortuin and P. W. Kasteleyn, Physica (Amsterdam) **57**, 536 (1972).
[17] A. M. Ferrenberg and R. H. Swendsen, Phys. Rev. Lett. **61**, 2635 (1988).
[18] P. Minnhagen, Rev. Mod. Phys. **59**, 1001 (1987).
[19] K. Binder, Z. Phys. B: Condens. Matter **43**, 119 (1981).
[20] T. Surungan, Y. Okabe, and Y. Tomita, J. Phys. A **37**, 4219 (2004).
[21] C. Yasuda, S. Todo, M. Matsumoto, and H. Takayama, Phys. Rev. B **64**, 092405 (2001).
[22] C. Yasuda, S. Todo, M. Matsumoto, and H. Takayama, J. Phys. Chem. Solids, **63**, 1607 (2002).
[23] T. Sasamoto and H. Nishimori, Prog. Theor. Phys. Suppl. (to be published).